Available online at www.sciencedirect.com
ScienceDirect
Journal of Organometallic Chemistry 691 (2006) 5655–5663
Journal of Organometallic Chemistry
www.elsevier.com/locate/jorganchem

μ-Coordination chemistry of NO ligands: Adducts of *trans*-Mo(dmpe)$_2$(H)(NO) with lithium salts

Fupei Liang [a], Helmut W. Schmalle [b], Heinz Berke [b,*]

[a] *School of Chemistry and Chemical Engineering, Guangxi Normal University, Guilin 541004, PR China*
[b] *Anorganisch-Chemisches Institut der Universität Zürich, Winterthurer strasse 190, CH-8057 Zürich, Switzerland*

Received 24 May 2006; received in revised form 11 August 2006; accepted 13 September 2006
Available online 19 September 2006

Abstract

Four adducts were formed by the reaction of *trans*-Mo(dmpe)$_2$(H)(NO) (**1**) (dmpe = bis(dimethylphosphino)ethane) and a respective lithium reagent to afford, [Mo(dmpe)$_2$(H)(NO)LiHBEt$_3$]$_2$ (**2**), [Mo(dmpe)$_2$(H)(NO)LiN(SiMe$_3$)$_2$]$_2$ (**3**), [Mo(dmpe)$_2$(H)(NO)]$_3$(LiBH$_4$)$_2$ (**4**), and {[Mo(dmpe)$_2$(H)(NO)]$_2$[LiBH$_4$]$_5$}$_n$ (**5**). Structures **2**–**5** were characterized by crystal X-ray diffraction analyses. Structures **2** and **3** revealed to be dimers of the 1:1 adduct of **1** and the lithium salt. The two nitrosyl oxygen atoms in **2** are μ$_2$-bridged connecting two separate LiHB(C$_2$H$_5$)$_3$ moieties, whereas in **3** these oxygen atoms exhibit a terminal coordination mode binding to two lithium ions of the dimeric [LiN(SiMe$_3$)$_2$]$_2$ unit. Structure **4** shows a discrete structure formed by two separate mononuclear LiBH$_4$ units being bridged by the nitrosyl oxygen atoms of three Mo(dmpe)$_2$(H)(NO) moieties. Structure **5** displays a complicated chain structure with differently coordinated lithium centers, various types of bridging BH$_4$ and bridging nitrosyl groups.

Keywords: Hydride; Nitrosyl binding; Molybdenum; Lithium; Adduct formation

1. Introduction

The Lewis basicity of coordinated carbonyl ligands has been well documented [1]. In contrast, studies on the interaction of bound NO acting as a Lewis base are relatively rare [2]. The first investigation on the Lewis basicity of the NO ligand was made by Legzdins and his coworkers. They studied the interaction of CpCr(NO)$_2$Cl and CpM(CO)$_2$(NO) (M = Cr, Mo, W) with R$_3$Ln (R = Cp, Cp′; Ln = Sm, Er, Yb, Ho, Dy) in solution by IR and NMR spectroscopy [3]. The Lewis basicity of the nitrosyl was indicated by IR and ^{1}H NMR spectroscopic changes accompanied by lowering of the *ν*(NO) frequencies, which occur upon adduct formation. Similar spectroscopic methods were used in the study of the interaction of Cp$_3$Sm in solution with CpCr(CO)$_2$(NO), [CpFe(NO)]$_2$ and Cp′$_3$Mn$_3$(NO)$_4$ that stand for three kinds of ligation modes of NO groups, namely, terminal, μ$_2$-bridging and μ$_3$-bridging, respectively. Based on the IR spectroscopic changes in the adduct formation, the Lewis basicity of the NO ligand was shown to have the order of terminal NO > μ$_2$–NO > μ$_3$–NO [4]. The MgI$_2$ complexes of CpM(NO)(CH$_2$SiMe$_3$) have been isolated in analytically pure form with the compositions of [CpM(NO)(CH$_2$SiMe$_3$)$_2$]$_2$ · MgI$_2$ · Et$_2$O (M = Mo, W) [5]. The existences of the isonitrosyl linkage (NO → Mg) in both complexes were manifested by IR spectroscopy and partially by X-ray crystallographic analyses of the complexes. The analogous complex CpMo(NO)I$_2$ · C$_4$H$_6$Mg · 1/2(Et$_2$O) has also been isolated and characterized.[6] The crystal structure of the nitrosyl ligand/Lewis acid adduct CpRe(NO · BCl$_3$) (PPh$_3$)(SiMe$_2$Cl) has been determined [7]. The Re–N bond is distinctly shortened and the N–O bond revealed lengthening upon the formation of the adduct. In dinitrosyl complexes Re(H)(NO)$_2$(PR$_3$)$_2$ (R = ^{i}Pr, Cy), one NO group was found to be capable of coordinating to one or two BF$_3$ molecules, and more interesting, the interaction of a second

* Corresponding author. Tel.: +41 1 635 46 80; fax: +41 1 635 68 02.
E-mail address: hberke@aci.unizh.ch (H. Berke).

0022-328X/$ - see front matter © 2006 Elsevier B.V. All rights reserved.
doi:10.1016/j.jorganchem.2006.09.016

BF_3 molecule caused bending of the NO group, thus providing a new coordination site in the metal sphere [8]. The coordination of the nitrosyl group to the lithium ions in the compounds $[Cp^*Mo(NO)(CH_2SiMe_3)(=CHSiMe_3)]_2[Li_2(THF)_3]$, $[(\eta^5,\eta^1\text{-}C_5Me_4CH_2)Mo(NO)(CH_2SiMe_3)_2][Li(THF)_3]$ and $\{[Cp^*Mo(NO)(CH_2SiMe_3)_2][Li(THF)]\}_2$ have been unambiguously confirmed by X-ray crystallographic analyses [9]. We have previously reported the structural characterizations of the compounds formed by the chloride *trans*-$Mo(dmpe)_2(Cl)(NO)$ (dmpe = bis(dimethylphosphino)ethane) and lithium reagents [10]. Extending these investigations, we present here structural characterizations of the adducts of the hydride *trans*-$Mo(dmpe)_2(H)(NO)$ (**1**) and various lithium salts.

2. Results and discussion

2.1. Preparation and characterization of complex 2–5

Complex **2**: Treatment of **1** with equimolar lithium triethylborohydride in diethyl ether afforded the **1**/$LiHBEt_3$ adduct $[Mo(dmpe)_2(H)(NO)LiHBEt_3]_2$ (**2**), which was isolated as well-defined crystals in 68% yield after diffusion of pentane into a concentrated toluene solution of the reaction mixture (Eq. (1)). The IR spectrum of **2** as a Nujol mull showed an ν(NO) absorption at 1520 cm^{-1} of medium intensity. This NO stretching frequency is 23 cm^{-1} lower than the corresponding one of the precursor **1** (1543 cm^{-1} in Nujol), suggesting interaction of the lithium cation at the nitrosyl oxygen atom. The ^1H and ^{13}C NMR spectra of **2** in Et_2O-d_{10} display the expected resonances corresponding to the $Mo(dmpe)_2H(NO)$ and $LiHBEt_3$ moieties. The signal for the Mo–H proton is observed at −4.75 ppm. This resonance is a little upfield from the related resonance of **1**. However, this effect is believed to be more due to a solvent effect rather than a consequence of the interaction with the lithium ion. The ^{31}P resonance is found at 44.2 ppm, which is the same as the spectrum of the precursor **1**. The ^{11}B NMR spectrum shows a singlet at −13.6 ppm, which is quite different from that observed in the adduct of $[Mo(dmpe)_2(Cl)(NO)LiHBEt_3]_n$ [10]. Despite this observation, the ^7Li spectra of both compounds are comparable, a singlet at 2.3 ppm is observed for **2**

$$z \cdot x\mathrm{Mo(dmpe)_2(H)(NO)} + z \cdot y\mathrm{LiX} \rightarrow \{[\mathrm{Mo(dmpe)_2(H)(NO)}]_x(\mathrm{LiX})_y\}_z \quad (1)$$

2 : $x = y = 1;\ z = 2;\ X = HBEt_3$

3 : $x = y = 1;\ z = 2;\ X = N(SiMe_3)_2$

4 : $x = 3;\ y = 2;\ z = 1;\ X = BH_4$

5 : $x = 2;\ y = 5;\ z = \infty;\ X = BH_4$

Complex **3**: Reaction of **1** with 1 equiv of lithium bis(trimethylsilyl)amide in diethyl ether at room temperature and recrystallization from diethyl ether afforded yellow crystals of $[Mo(dmpe)_2(H)(NO)LiN(SiMe_3)_2]_2$ (**3**) in 81% yield (Eq. (1)). **3** has been characterized by elemental analysis, IR and NMR. The analysis data are in good agreement with the 1:1 stoichiometry of **1**/$LiN(SiMe_3)_2$. The IR spectrum as a Nujol mull shows the nitrosyl stretching mode at 1528 cm^{-1}, which is 15 cm^{-1} lower than that found for precursor **1**. The extent of the decrease of ν_{NO} is for **3** apparently smaller than that of **2**, which is the consequence of the non-bridging coordination mode of the nitrosyl oxygen in **3** (*vide infra*). The ^1H and ^{13}C NMR spectra in Et_2O-d_{10} display the expected resonances corresponding to the $Mo(dmpe)_2H(NO)$ and $LiN(SiMe_3)_2$ moieties. The chemical shifts of −4.75 ppm for the Mo–H proton resonance (^1H NMR) and 44.7 ppm for the ^{31}P resonance (^{31}P NMR) are comparable to those exhibited by **2**. In the ^7Li NMR spectrum the ^7Li resonance appears at 4.0 ppm.

Complex **4**: Treatment of **1** with $LiBH_4$ at room temperature in diethyl ether afforded the adduct $[Mo(dmpe)_2(H)(NO)]_3(LiBH_4)_2$ (**4**) with a **1**/$LiBH_4$ ratio of 3:2 (Eq. (1)). It was found that this stoichiometry is independent on the **1**/$LiBH_4$ ratio employed in the reaction. Reactions of **1** with 1 equiv or with 6 equiv of $LiBH_4$ produced the same compound of **4**. In a typical reaction, **4** was isolated as yellow crystals in 67% yield. The IR spectrum of **4** as Nujol mull shows the nitrosyl stretching mode at 1497 cm^{-1}. This value is 44 cm^{-1} lower than that of the precursor **1**. It is noteworthy that the extent of this ν_{NO} shift is significantly greater than those exhibited by **2** and **3**, which suggests an even stronger NO–Li interaction in **4**. Surprisingly the ^1H NMR spectrum of **4** displays in Et_2O-d_{10} among others characteristic resonances at −0.22 to −0.70 ppm for the BH_4^- group and a quintet at −4.78 ppm for the Mo–H resonance. A broad quartet at −2.95 ppm with a coupling constant of 80.4 Hz is assigned to the previously reported borohydride *trans*-$Mo(\eta^1\text{-}BH_4)(dmpe)_2(NO)$ [11]. Accordingly, the $^{31}P\{^1H\}$ and $^{11}B\{^1H\}$ NMR spectra of **4** show also additional resonances corresponding to the borohydride species (36.5 ppm and −43.0 ppm, respectively). This indicates the appearance of *trans*-$Mo(\eta^1\text{-}BH_4)(dmpe)_2(NO)$ in the diethyl ether solution of **4**. We assume that **4** dissociates in Et_2O into the corresponding components of the hydride **1** and $LiBH_4$. And then hydride **1** is assumed to react with $LiBH_4$ in an equilibrium to form slowly the borohydride and LiH (Eq. (2)). This assumption could be confirmed by NMR. The ^1H and ^{31}P NMR spectra recorded from the mixture of **1** and $LiBH_4$ in Et_2O-d_{10} show indeed the occurrence of the borohydride *trans*-$Mo(\eta^1\text{-}BH_4)(dmpe)_2(NO)$. The $^7Li\{^1H\}$ NMR spectrum of **4** in Et_2O-d_{10} displays only a singlet at 3.2 ppm for $LiBH_4$ (3.3 ppm, recorded in Et_2O-d_{10}). The other product LiH could not be traced due to its insolubility in ether.

$$\mathbf{1} + \mathrm{LiBH_4} \rightarrow \textit{trans}\text{-}\mathrm{Mo}(\eta^1\text{-}\mathrm{BH_4})(\mathrm{dmpe})_2(\mathrm{NO}) + \mathrm{LiH} \quad (2)$$

Complex **5**: Reaction of the chloride *trans*-$Mo(dmpe)_2(Cl)(NO)$ with 5 equiv of $LiBH_4$ and 8 equiv of quinuclidine in Et_2O at room temperature for four days and subsequent treatment produced unexpectedly a poly-

meric **1**/$LiBH_4$ adduct $\{[Mo(dmpe)_2(H)(NO)]_2[LiBH_4]_5\}_\infty$ (**5**) (Eq. (1)). Unfortunately, we failed to isolate an analytically pure sample of **5** for elemental analysis and spectroscopic characterization, apparently because of the coexistence of **5** and some other unknown solid compounds. But the composition and the structure of **5** could be recurred by an single crystal X-ray diffraction analysis.

2.2. Structures of 2–5

Structure of **2**: An ORTEP drawing of **2** is given in Fig. 1. The structure shows clearly **2** as a $[Mo(dmpe)_2(H)(NO)LiHB(C_2H_5)_3]_2$ adduct, a dimer of a 1:1 **1**/$LiHB(C_2H_5)_3$ composition. Two $Mo(dmpe)_2H(NO)$ moieties act as μ_2-bridging ligands connecting two separate $LiHB(C_2H_5)_3$ units via two oxygen atoms of the nitrosyl groups. The H_{Mo} atom did not reveal coordination with the lithium ion despite the great affinity of lithium ions to H^- or hydridic hydrogen atoms. Each lithium ion is tricoordinated in a distorted trigonal planar arrangement accommodating two bridging oxygen atoms and one hydrogen of the $[HBEt_3]^-$ anion. The four-membered $(LiO)_2$ ring is planar. The average Li–O distance of 1.934(10) Å (Table 1) is comparable to that found in the previously reported *trans*-$Mo(dmpe)_2(Cl)(NO)/LiHBEt_3$ adduct [10]. Although this value is significantly shorter than that of 2.040(10) Å for the *trans*-$Mo(dmpe)_2(Cl)(NO)$/LiI adduct, which exhibits a similar binding mode for the oxygen atoms [10], it does not bring the two lithium ions closer together. The Li–Li distance of 2.716(14) Å in **2** is much longer than the value of 2.38(3) Å of the *trans*-$Mo(dmpe)_2(Cl)(NO)$/LiI adduct, presumably due to the greater steric repulsion between the $[B(C_2H_5)_3]$ and the $[Mo(dmpe)_2H]$ residues. The average Li–H distance is 1.718(10) Å. The average Mo–N distance of 1.761(4) Å is shorter than those found in the *trans*-$Mo(dmpe)_2(Cl)(NO)/LiHB(C_2H_5)_3$ adduct, whereas the average N–O distance of 1.274(5) Å is longer, which suggests an even stronger Mo → NO back-bonding in **2**. Unfortunately there are no structural data of **1** for comparison, because of the failure to obtain suitable single crystals. However, shortening of the Mo–N bond and lengthening of the N–O bond from the precursor **1** to the adduct **2** are expected to occur due to the interaction of the lithium ion with the nitrosyl moiety. The Mo1–H1

Table 1
Selected bond lengths [Å] and bond angles [°] of **2**

Bond lengths		Bond angles	
Mo(1)–N(1)	1.756(4)	N(1)–Mo(1)–P(1)	96.30(12)
Mo(1)–P(1)	2.4457(14)	N(1)–Mo(1)–P(2)	98.67(14)
Mo(1)–P(2)	2.4561(17)	N(1)–Mo(1)–P(3)	97.58(14)
Mo(1)–P(3)	2.4331(17)	N(1)–Mo(1)–P(4)	99.60(12)
Mo(1)–P(4)	2.4468(14)	P(1)–Mo(1)–P(2)	80.34(5)
Mo(1)–H(1)	2.07(2)	P(3)–Mo(1)–P(4)	80.49(5)
N(1)–O(1)	1.268(4)	H(1)–Mo(1)–P(1)	84.3(12)
O(1)–Li(1)	1.949(10)	H(1)–Mo(1)–P(2)	83.7(14)
O(1)–Li(2)	1.944(9)	H(1)–Mo(1)–P(3)	80.0(14)
Li(1)–Li(2)	2.716(14)	H(1)–Mo(1)–P(4)	79.9(12)
Li(1)–H(3)	1.705	N(1)–O(1)–Li(1)	142.4(4)
B(1)–H(3)	1.220	N(1)–O(1)–Li(2)	126.5(4)
Mo(2)–N(2)	1.765(4)	Li(1)–O(1)–Li(2)	88.5(4)
Mo(2)–P(5)	2.4478(14)	O(1)–Li(1)–O(2)	85.4(4)
Mo(2)–P(6)	2.4494(14)	O(1)–Li(1)–H(3)	164.3
Mo(2)–P(7)	2.4415(16)	O(2)–Li(1)–H(3)	110.3
Mo(2)–P(8)	2.4396(16)	O(1)–Li(2)–O(2)	86.7(5)
Mo(2)–H(2)	1.86(2)	O(1)–Li(2)–H(4)	109.0
N(2)–O(2)	1.280(5)	O(2)–Li(2)–H(4)	162.8
O(2)–Li(1)	1.942(9)	Li(1)–O(2)–Li(2)	89.9(4)
O(2)–Li(2)	1.901(12)	N(2)–O(2)–Li(1)	130.6(5)
Li(2)–H(4)	1.730	N(2)–O(2)–Li(2)	138.8(4)
B(2)–H(4)	1.189	Mo(1)–N(1)–O(1)	175.6(4)

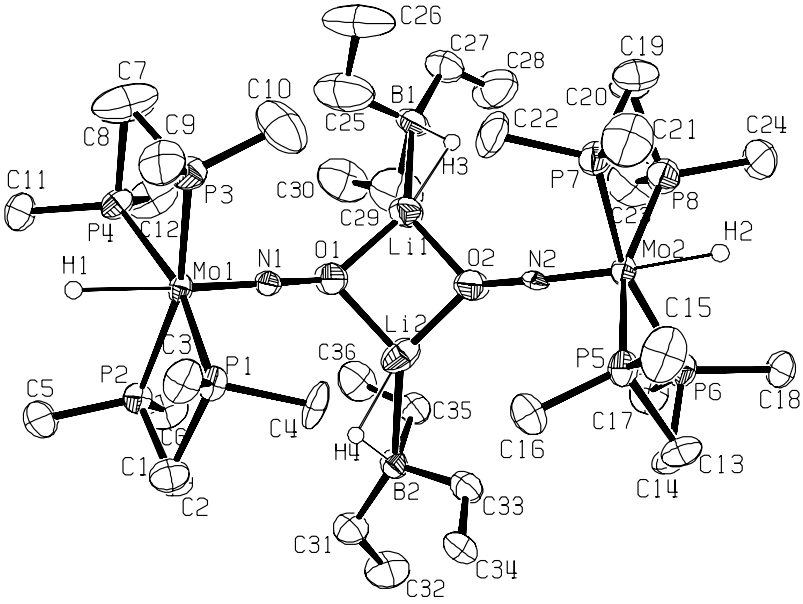

Fig. 1. ORTEP plot of the structure of **2**. Displacement ellipsoids are drawn with 50% probability.

and Mo2–H2 distances are found to be 2.07(2) Å and 1.86(2) Å, respectively, which are surprisingly different. However, considering the generally high standard deviations for hydrogen positions in X-ray diffraction analyses, the meaning of any bond length comparison of the Mo–H bond distances of **2** is questionable. Analyzing related bond angles, we can conclude that the dmpe ligands bend to the side of the hydride atom. The Mo–P bond distances in **2** are apparently not affected by this, because they are almost the same as those found in the chloride *trans*-$Mo(dmpe)_2(Cl)(NO)$.

Structure of **3**: The unit cell of **3** contains two independent molecules. One molecule could be properly refined. The other one displayed disorder in the $[N(SiMe_3)_2]^-$ groups and the two PMe residues of the dmpe ligands. Fig. 2 shows a structural model of **3**. Selected bond distances and angles of the two independent molecules are given in Table 2. The X-ray structure reveals a dimeric unit with a 1:1 composition of **3** according to the formula $[Mo(dmpe)_2H(NO)LiN(SiMe_3)_2]_2$. The 1:1 adduct stoichiometry of **3** is similar to that of **2**. However, the coordination of the "$Mo(dmpe)_2(H)(NO)$" ligand and the aggregation modes of the lithium-containing moieties differ greatly from each other. In contrast to the formation of discrete units in the case of **2**, the lithium-containing moieties in **3** form a dimer via amide bridges. The $Mo(dmpe)_2H(NO)$ moieties act as terminal "ligands", unlike the bridging function in **2** coordinating via nitrosyl oxygen atoms to the dimeric $[LiN(SiMe_3)_2]_2$ unit to complete the three-coordinate lithium environment. Such a dimeric structure for **3** is comparable to those observed in $[Li(Et_2O)N(SiMe_3)_2]_2$ [12] and $[Li(THF)N(SiMe_3)_2]_2$ [13], where the $Mo(dmpe)_2H(NO)$ unit plays the role as the solvate molecules Et_2O or THF. The four-membered $(LiN)_2$ ring is planar, the average Li–N, Li–Li distances and N–Li–N, Li–N–Li angles related to the $(LiN)_2$ ring in **3** (Table 2) do not show significant differences to those in $[Li(Et_2O)N(SiMe_3)_2]_2$ [12] and $[Li(THF)N(SiMe_3)_2]_2$ [13], indicating less influence on the dimeric $[LiN(SiMe_3)_2]_2$ unit of the "complex ligand" in comparison with other solvate molecules. The average O–Li distances of 1.807(12) and 1.831(13) Å are distinctly shorter than those found in **2** (av. 1.934(10) Å), which is consistent with the fact that the nitrosyl oxygen atom possesses a terminal (**3**) rather than a bridging (**2**) function. For the $Mo(dmpe)_2H(NO)$ moiety, the average Mo–N distances in **3** are found to be 1.790(6) and 1.789(7) Å, which both being longer than that in **2** (1.761(4) Å), whereas the average N–O distances of 1.226(8) and 1.206(9) Å are shorter than the value of 1.274(5) Å of **2**. These results suggest that the Mo → NO back-bonding is weaker in **3** than in **2**. Although both Mo → NO bonds in **3** and **2** are assumed to be strengthened due to the interaction of the nitrosyl oxygen with the lithium ion in comparison with the precursor **1**, the terminal coordination mode of the nitrosyl oxygen apparently

Table 2
Selected bond lengths [Å] and bond angles [°] of **3**

Bond lengths		Bond angles	
Mo(1)–N(1)	1.799(6)	N(1)–Mo(1)–P(1)	97.7(2)
Mo(1)–P(1)	2.437(2)	N(1)–Mo(1)–P(2)	97.6(2)
Mo(1)–P(2)	2.433(2)	N(1)–Mo(1)–P(3)	97.4(2)
Mo(1)–P(3)	2.4420(19)	N(1)–Mo(1)–P(4)	97.3(2)
Mo(1)–P(4)	2.443(2)	P(1)–Mo(1)–P(2)	80.57(7)
Mo(1)–H(1)	1.854	P(3)–Mo(1)–P(4)	80.03(7)
N(1)–O(1)	1.207(9)	H(1)–Mo(1)–P(1)	72.88
O(1)–Li(1)	1.814(13)	H(1)–Mo(1)–P(2)	84.42
N(3)–Li(1)	2.062(15)	H(1)–Mo(1)–P(3)	81.07
N(4)–Li(1)	2.024(13)	H(1)–Mo(1)–P(4)	92.17
Li(1)–Li(2)	2.467(18)	N(1)–Mo(1)–H(1)	170.0
Mo(2)–N(2)	1.781(6)	N(1)–O(1)–Li(1)	176.0(9)
Mo(2)–P(5)	2.426(2)	O(1)–Li(1)–N(3)	126.7(7)
Mo(2)–P(6)	2.424(2)	O(1)–Li(1)–N(4)	128.9(8)
Mo(2)–P(7)	2.443(2)	N(3)–Li(1)–N(4)	104.2(6)
Mo(2)–P(8)	2.434(2)	O(2)–Li(2)–N(3)	128.4(8)
Mo(2)–H(2)	1.913	O(2)–Li(2)–N(4)	125.5(7)
N(2)–O(2)	1.244(9)	N(3)–Li(2)–N(4)	106.1(6)
O(2)–Li(2)	1.799(14)	N(2)–O(2)–Li(2)	172.8(9)
N(3)–Li(2)	2.012(13)	Li(1)–N(3)–Li(2)	74.5(5)
N(4)–Li(2)	2.022(14)	Mo(1)–N(1)–O(1)	177.8(7)

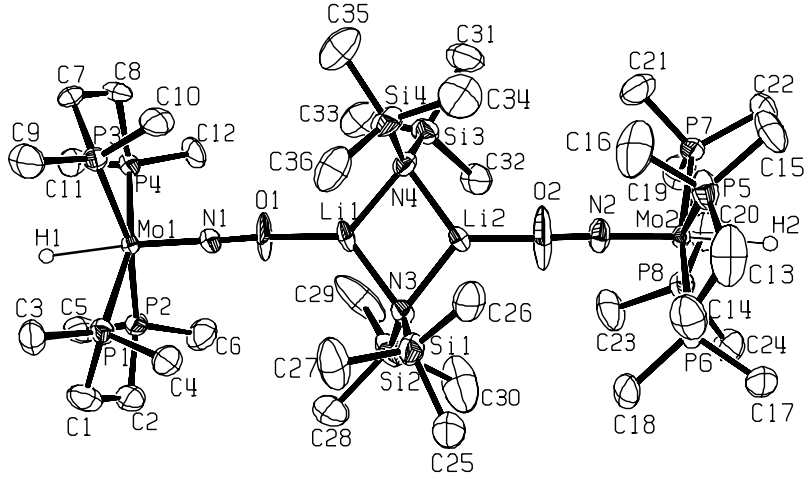

Fig. 2. ORTEP plot of the structure of **3**. Only one molecule in the unit cell is shown. Displacement ellipsoids are drawn with 50% probability.

brings about less Mo → NO back-bonding. The hydride atom of **1** is not involved in the interaction with lithium ion. Like in the case of **2**, the dmpe ligands bend in **3** toward the hydride atom presumably due to steric repulsion between the [$N(SiMe_3)_2$] residues and the dmpe ligands.

Structure of **4**: An ORTEP drawing of **4** is shown in Fig. 3, and selected bond lengths and angles are given in Table 3. Although the dimethylphosphinoethane ligands show disorder, the nitrosyl group and the $LiBH_4$ moieties are not affected by this and clearly demonstrate interaction. Surprisingly, the structure of **4** is quite similar to that of the *trans*-Mo(dmpe)$_2$(Cl)(NO)/LiI adduct [10]. There is no bridging between the two Li centers by the BH_4^- group. Two discrete monomeric $LiBH_4$ units are connected by bridging O_{NO} atoms of three "Mo(dmpe)$_2$(H)(NO) ligands". In each mononuclear $LiBH_4$ unit, the BH_4^- group binds in a η^3-bonding mode to a lithium ion. Previously only a few $LiBH_4$/Lewis base structures have been structurally characterized [14,15]. In the reported $LiBH_4$/Lewis base adducts containing two $LiBH_4$ units, the BH_4^- groups act as bridging ligands in most cases to link the two Li centers through their μ_2- or μ_3-bridging hydrogens [15]. The terminal binding mode of the BH_4^- groups as in **4** has been found only in one case with a crown ether as ligand [16]. Apparently the presence of the structural feature of the terminal binding mode of the BH_4^- groups in **4** is attributed to the competition between the BH_4^- and the "Mo(dmpe)$_2$(H)(NO) ligand" bridges. The lithium centers in **4** can be viewed as six-coordinate with three hydrogen atoms of the BH_4^- group and three μ-oxygen atoms of the "Mo(dmpe)$_2$(H)(NO) ligands". The Li–H bond length of 2.02(10) Å is comparable to the Li-(μ_2–H) distances found in [TMEDA · $LiBH_4$]$_2$ (2.02(3) and 2.06(4) Å) [15a]. The Li–B distance of 2.31(2) Å is shorter than those observed in [TMEDA · $LiBH_4$]$_2$ (av. 2.464(6) Å) and in [($MeOCH_2CH_2OMe$)3Li(μ-H)$_2$B(2,4,6-$C_6H_2Me_3$)$_2$] (2.49(4) Å) [17], but it is not especially short when compared with the value of 2.19(4) Å of the monomeric complex (THF)$_3$Li(μ-H)$_3$BC($SiMe_2Ph$)$_3$ [18]. The Li–Li distance is 2.63(3) Å, which is a significantly closer contact than that in [TMEDA · $LiBH_4$]$_2$ (3.089(9) Å). Such a shortening of the Li–Li distance is not unexpected for complexes featuring special ligand bridges [10,19]. The O–Li bond length of 2.069(10) Å in **4** is significantly longer than that observed in [Mo(dmpe)$_2$(Cl)(NO)LiHB(C_2H_5)$_3$]$_n$ (av. 1.934(10) Å [10]) which bears also a μ_2-oxygen bridge. This is attributed to a steric effect due to the higher coordination number around the lithium in **4**. The average Mo–N distance of

Table 3
Selected bond lengths [Å] and bond angles [°] of **4**

Bond lengths		Bond angles	
Mo(1)–N(1)	1.789(6)	N(1)–Mo(1)–P(1)	98.05(13)
Mo(1)–P(1)	2.4302(19)	N(1)–Mo(1)–P(2)	97.60(13)
Mo(1)–P(2)	2.4173(19)	P(1)–Mo(1)–P(2)	87.53(10)
Mo(1)–H(1)	2.02(6)	H(1)–Mo(1)–P(1)	79.2(12)
N(1)–O(1)	1.261(7)	H(1)–Mo(1)–P(2)	85.2(13)
O(1)–Li(1)	2.069(10)	N(1)–O(1)–Li(1)	129.6(3)
Li(1)–H(2)	2.02(10)	Li(1)–O(1)–Li(1)	78.6(6)
Li(1)–Li(1)	2.62(3)	O(1)–Li(1)–O(1)	84.1(5)
Li(1)–B(1)	2.31(2)	O(1)–Li(1)–B(1)	129.3(3)
B(1)–H(2)	1.22(11)	N(1)–Mo(1)–H(1)	176.1(18)
B(1)–H(3)	1.2(2)	O(1)–N(1)–Mo(1)	179.9(4)

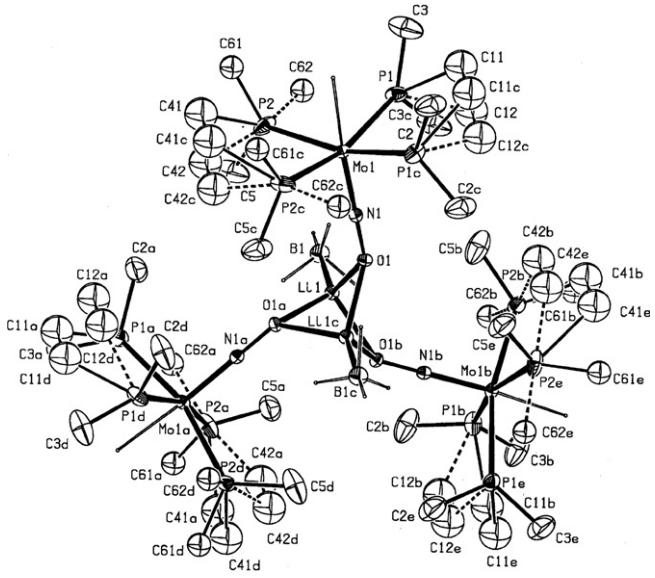

Fig. 3. ORTEP plot of the structure of **4**. Displacement ellipsoids are drawn with 50% probability.

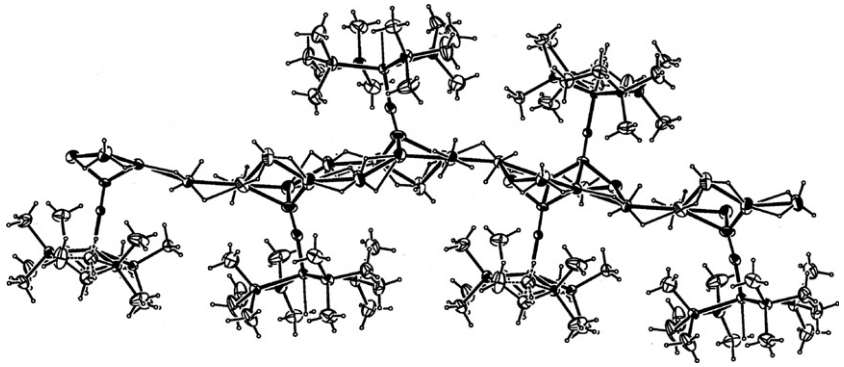

Fig. 4. A structural fragment of **5**.

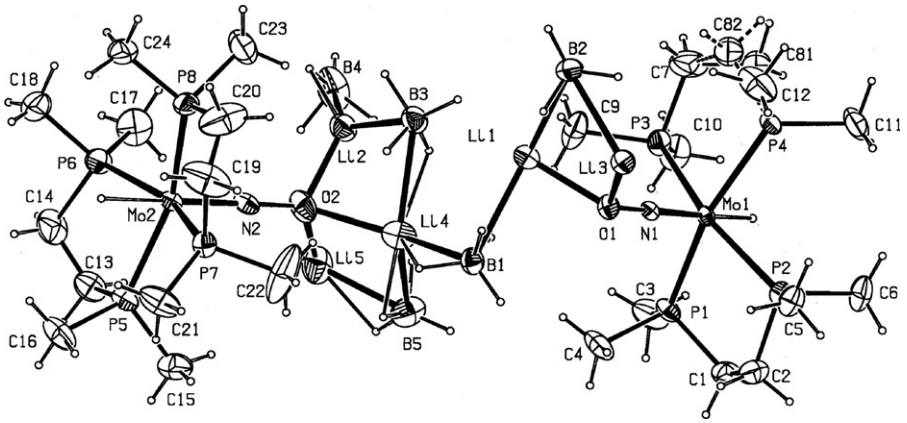

Fig. 5. The structure of an asymmetric unit of **5**. Displacement ellipsoids are drawn with 50% probability.

1.789(6) Å in **4** is longer than that in **2** (1.761(4) Å), and the N–O distance of 1.261(7) Å is shorter compared with the value of 1.274(5) Å of **2** indicating a weaker Mo → NO back-bonding in **4**. In contrast to the comparable Mo–N distance in **3**, the N–O distance of **4** is unusually long (1.226(8) and 1.206(9) Å in **3**).

Structure of **5**: As a whole, **5** adopts a complicated chain structure. A fragment of this infinite chain is shown in Fig. 4. The basic structural motif of **5** is illustrated in Fig. 5. The infinite chain is assembled by connecting the basic structural units through six atoms: Li3 (Fig. 5) is connected by O1(i_1) and B1(i_1) of another unit; B4 and Li5 link to Li5(i_3) and B4(i_3) of another unit; O1 and B1 connect to Li3(i_2) and Li3(i_1); and Li4 is linked by B1(i_4) [i_1, i_2, i_3, and i_4 represent the following symmetry operations: $i_1 = -x+1, -y+1, -z+1$; $i_2 = x, y, z+1$; $i_3 = -x, -y, -z$; $i_4 = x, y, z-1$]. This structure exhibits several interesting features. First, the lithium ions in one unit show different coordination environments. Li3 and Li4 (Fig. 5) are tetracoordinate, while Li1, Li2 and Li5 are tricoordinate (considering B, not the H atoms of BH_4 group as coordination partners). Second, the BH_4 groups show different bridging modes. The BH_4 groups of B2, B3, B4 and B5 act as μ_2-bridges for two lithium ions, whereas the BH_4 group of B1 acts as a μ_3-bridging coordinating to three lithium ions. The μ_3 mode of the BH_4 group presented here has not been reported elsewhere for the $LiBH_4$ complexes, although it has been observed in a $NaBH_4$ complex [15b]. Third, the nitrosyl oxygen atom coordinates to three lithium ions in a μ_3-bridging mode. It is again the first case to observe a μ_3-bridging mode for the O_{NO} atom. This μ_3-O_{NO} group of **5** causes the longest N–O bond length (1.284(2) and 1.299(3) Å, Table 4) among all nitrosyl/lithium salt adducts.

Table 4
Selected bond lengths [Å] and bond angles [°] of **5**

Bond lengths		Bond angles	
Mo(1)–N(1)	1.7816(18)	N(1)–Mo(1)–P(1)	99.64(7)
Mo(1)–P(1)	2.4303(8)	N(1)–Mo(1)–P(2)	101.04(6)
Mo(1)–P(2)	2.4515(7)	N(1)–Mo(1)–P(3)	99.78(6)
Mo(1)–P(3)	2.4491(7)	N(1)–Mo(1)–P(4)	101.00(7)
Mo(1)–P(4)	2.4480(8)	P(1)–Mo(1)–P(2)	79.99(3)
Mo(1)–H(1)	1.660(19)	P(3)–Mo(1)–P(4)	80.06(3)
N(1)–O(1)	1.284(2)	H(1)–Mo(1)–P(1)	78.9(11)
O(1)–Li(1)	2.075(5)	H(1)–Mo(1)–P(2)	84.4(11)
O(1)–Li(3)	2.006(5)	H(1)–Mo(1)–P(3)	74.7(11)
Mo(2)–H(2)	1.82(3)	H(1)–Mo(1)–P(4)	80.5(11)
N(2)–O(2)	1.299(3)	H(1)–Mo(1)–N(1)	174.1(10)
O(2)–Li(2)	1.939(6)	O(1)–N(1)–Mo(1)	178.35(16)
O(2)–Li(4)	2.375(6)	N(1)–O(1)–Li(3)	123.14(18)
O(2)–Li(5)	1.946(7)	N(1)–O(1)–Li(1)	118.11(19)
B(1)–Li(1)	2.504(6)	Li(3)–O(1)–Li(1)	93.0(2)
B(1)–Li(4i_2)	2.453(6)	N(2)–O(2)–Li(2)	116.8(2)
B(2)–Li(3)	2.423(6)	N(2)–O(2)–Li(5)	117.1(2)
B(2)–Li(1)	2.462(7)	N(2)–O(2)–Li(4)	130.3(2)
B(3)–Li(2)	2.331(6)	O(1)–Li(1)–B(2)	88.7(2)
B(3)–Li(4)	2.501(7)	O(1)–Li(1)–B(1)	86.0(2)
B(4)–Li(2)	2.223(6)	B(2)–Li(1)–B(1)	147.0(2)
B(5)–Li(4)	2.411(7)	O(2)–Li(2)–B(4)	118.5(3)
B(5)–Li(5)	2.300(7)	O(2)–Li(2)–B(3)	100.8(2)
O(1)–Li(3i_1)	2.011(5)	B(3)–Li(2)–B(4)	137.4(3)
B(1)–Li(3i_1)	2.410(5)	O(1)–Li(3)–B(2)	91.4(2)
Li(3)–O(1i_1)	2.011(5)	O(2)–Li(4)–B(5)	85.7(2)
Li(3)–B(1i_1)	2.410(5)	O(2)–Li(4)–B(3)	85.2(2)
B(4)–Li(5i_3)	2.352(7)	B(5)–Li(4)–B(3)	138.8(3)
Li(5)–B(4i_3)	2.352(7)	O(2)–Li(5)–B(5)	99.8(3)
Li(4)–B(1i_4)	2.453(6)	O(2)–N(2)–Mo(2)	174.39(18)

Symmetry operations: $i_1 = -x+1, -y+1, -z+1$; $i_2 = x, y, z+1$; $i_3 = -x, -y, -z$; $i_4 = x, y, z-1$.

3. Conclusions

In summary, the reactions of the hydride Mo(dmpe)$_2$(H)(NO) **1** with the lithium reagents $LiHB(C_2H_5)_3$ and $LiN(SiMe_3)_2$ afford **1**/lithium reagent adducts, which are based on the coordination of the nitrosyl group to the lithium ion. For $LiBH_4$, even two **1**/$LiBH_4$ compounds with different compositions and structures are obtained. The formation of these adducts demonstrates a relatively strong donicity effect of the nitrosyl group in **1**, which in turn is for the most part a consequence of the strongly σ-donating property of the dmpe ligand. The two dmpe ligands in **1** increase the electron density on the molybdenum center, thus enhance concomitantly the electron density on the O_{NO} atom via back bonding

of the NO ligand. The resulting high propensity of the O_{NO} atom to act as a σ-donor may even have implications for the reactivity of the parent hydride, especially for the formation of dihydrogen bonds and in ionic hydrogenation catalyses.

4. Experimental section

All reactions and manipulations were performed under an atmosphere of dry nitrogen using conventional Schlenk techniques or a glovebox. Solvents were dried by standard methods and freshly distilled under nitrogen before use. *trans*-Mo(dmpe)$_2$(Cl)(NO) and *trans*-Mo(dmpe)$_2$(H)(NO) (**1**) were prepared as described previously [11]. Other reagents were purchased from Fluka or Aldrich. NMR spectra were recorded on the following spectrometers: Varian Gemini-300 instrument, ^{1}H at 300.1 MHz, ^{13}C at 75.4 MHz, ^{31}P at 121.5 MHz, ^{11}B at 96.2 MHz; Bruker DRX-500 instrument, ^{7}Li at 194.4 MHz. $\delta(^1H)$ and $\delta(^{13}C)$ are relative to $SiMe_4$, $\delta(^{31}P)$ is relative to 85% H_3PO_4, $\delta(^{11}B)$ is relative to $BF_3 \cdot OEt_2$, and $\delta(^7Li)$ is relative to $LiClO_4$ in H_2O. IR spectra were recorded on a Biorad FTS-45 instrument. Elemental analyses were performed on a Leco CHN(S)-932 instrument.

[Mo(dmpe)$_2$(H)(NO)LiHBEt$_3$]$_2$ **(2)**. To a solution of 0.025 g (0.059 mmol) of **1** in 10 mL of diethyl ether was added 0.06 ml (0.06 mmol) of lithium triethylborohydride solution (1.0 M solution in THF). The resulting solution was stirred overnight. Then the solvent was removed in vacuo. The remaining residue was extracted with toluene. Concentration of the combined extracts and diffusion of pentane into the solution afforded yellow crystals of **2**. Yield: 0.021 g (68%). IR (cm^{-1}, Nujol): 1520 (NO). ^{1}H NMR (Et$_2$O-d_{10}): 1.60 (m, 8H, PCH_2), 1.50 (s, 12H, PMe), 1.37 (s, 12H, PMe′), 0.75 (t, 9H, Me of BEt_3), 0.05 (br, 6H, CH_2 of BEt_3), −4.75 (quint, 1H, MoH). ^{13}C{^{1}H} NMR (Et$_2$O-d_{10}): 32.4 (quint, $^1J_{CP} = 9.8$ Hz, PCH_2), 22.9 (quint, $^1J_{CP} = 4.9$ Hz, PMe), 18.3 (quint, $^1J_{CP} = 4.9$ Hz, PMe′), 12.9 (br, Me of BEt_3). The resonances for CH_2 of BEt_3 overlapped with those of solvent. ^{31}P{^{1}H} NMR (Et$_2$O-d_{10}): 44.2 (s). ^{11}B NMR (Et$_2$O-d_{10}): −13.6 (s, br) ^{7}Li NMR (Et$_2$O-d_{10}): 2.3 (s). Anal. Calc. for $C_{18}H_{49}BLiMoNOP_4$: C, 40.54; H, 9.28; N, 2.63. Found: C, 41.04; H, 9.03; N, 2.41%.

[Mo(dmpe)$_2$(H)(NO)LiN(SiMe$_3$)$_2$]$_2$ **(3)**. A mixture of 0.022 g (0.051 mmol) of **1** and 0.0095 g (0.057 mmol) of lithium bis(trimethylsilyl)amide was dissolved in 15 mL of diethyl ether. The resulting solution was stirred overnight. Then the solvent was evaporated slowly at room temperature for several days to afford **3** as yellow crystals. Yield: 0.025 g (81%). IR (cm^{-1}, Nujol): 1528 (NO). ^{1}H NMR (Et$_2$O-d_{10}): 1.58 (m, 8H, PCH_2), 1.50 (s, 12H, PMe), 1.39 (s, 12H, PMe′), −0.06 (s, 18H, $SiMe_3$), −4.75 (quint, 1H, MoH). ^{13}C{^{1}H} NMR (Et$_2$O-d_{10}): 32.5 (quint, $^1J_{CP} = 9.7$ Hz, PCH_2), 23.0 (quint, $^1J_{CP} = 4.7$ Hz, PMe), 18.3 (m, PMe′), 6.2 (s, $SiMe_3$). ^{31}P{^{1}H} NMR (Et$_2$O-d_{10}): 44.7 (s). ^{7}Li NMR (Et$_2$O-d_{10}): 4.0 (s). Anal. Calc. for $C_{36}H_{102}Li_2Mo_2N_4O_2P_8Si_4$: C, 36.35; H, 8.66; N, 4.71. Found: C, 36.52; H, 8.59; N, 4.75%.

[Mo(dmpe)$_2$(H)(NO)]$_3$[LiBH$_4$]$_2$ **(4)**. A suspension of 0.026 g (0.061 mmol) of **1** and 0.008 g (0.37 mmol) of lithium borohydride in 15 mL of diethyl ether was stirred at room temperature for 4 days. Then the solvent was removed in vacuo. The residue was extracted with toluene until the solution remained colorless. The solvent of combined extracts was evaporated in vacuo and the remaining solid was redissolved in diethyl ether. Slow evaporation of diethyl ether at room temperature for several days afforded **4** as yellow crystals. Yield: 0.018 g (67%). IR (cm^{-1}, Nujol): 1497 (NO). ^{1}H NMR (Et$_2$O-d_{10}): 1.57 (m, PCH_2), 1.46 (s, PMe), 1.37 (s, PMe′), −0.22 ∼ −0.70 (m, $LiBH_4$), −2.95 (quart, br, Mo–HBH_3), −4.78 (quint, MoH). ^{13}C{^{1}H} NMR (Et$_2$O-d_{10}): 32.6 (quint, $^1J_{CP} = 10$ Hz, PCH_2), 23.2 (quint, $^1J_{CP} = 4.9$ Hz, PMe), 18.1 (quint, $^1J_{CP} = 4.9$ Hz, PMe′). ^{31}P{^{1}H} NMR (Et$_2$O-d_{10}): 44.9 (s), 36.5 (s). ^{11}B NMR (Et$_2$O-d_{10}): −40.4 (s), −43.0 (s, Mo–BH_4) ^{7}Li NMR (Et$_2$O-d_{10}): 3.2 (s). Anal. Calc. for $C_{36}H_{107}B_2Li_2Mo_3N_3O_3P_{12}$: C, 32.62; H, 8.15; N, 3.17. Found: C, 32.54; H, 8.19; N, 3.03%.

{[Mo(dmpe)$_2$(H)(NO)]$_2$[LiBH$_4$]$_5$}$_n$ **(5)**. A suspension of 0.056 g (0.12 mmol) of *trans*-Mo(dmpe)$_2$(Cl)(NO), 0.014 g (0.64 mmol) of lithium borohydride and 0.110 g (0.99 mmol) of quinuclidine in 20 mL of diethyl ether was stirred at room temperature. After 4 days the solvent was removed in vacuo. The remaining solid was washed with pentane and dried, and then dissolved in toluene. Diffusion of pentane into the toluene solution provided yellow crystals of **5** together with some unknown solid compounds. The single crystal suitable for X-ray diffraction study could be selected from the mixture, however, we failed to isolate an analytically pure sample for further characterization of elemental analyses, NMR, etc.

X-ray crystal structure analyses. The X-ray diffraction data were collected at 183(2) K (**2**, **4**), 173(2) K (**5**), and 123(2) K (**3**) using an imaging plate detector system (Stoe IPDS) with graphite monochromated MoK_α radiation. A total of 210, 238, 167, and 150 images were exposed at constant times of 5.00, 2.40, 1.50 and 4.00 min/image for compounds **2**–**4** and **5**, respectively. The crystal-to-image distances were set to 60, 88, 50 and 50 mm. The corresponding θ_{max} values were 27.95°, 22.62°, 30.39° and 30.29°, respectively. ϕ-oscillation (**2**, **3**, **5**) or rotation scan modes (**4**) were selected for the ϕ increments of 1.0°, 0.8°, 1.2° and 1.2° per exposure in each case. Total exposure times for the four compounds were 32, 26, 16, and 20 h. After integrations and corrections for Lorentz and polarization effects, a total of 8000 reflections (7998 for **4**) were selected out of the whole limiting sphere for the cell parameter refinements. A total of 29851, 31733, 39938, and 27070 reflections were collected, of which 13056, 16136, 3474, and 14159 reflections were unique ($R_{int} = 7.45\%$, 5.29%, 4.12%, and 4.54%); data reduction and numerical absorption correction used 16, 15, 17, and 12 indexed crystal faces [20]. The structures were solved by Patterson

Table 5
Crystallographic data and structure refinement parameters for **2**–**5**

	2	**3**	**4**	**5**
Formula	$C_{18}H_{49}BLiMoNOP_4$	$C_{36}H_{102}Li_2Mo_2\ N_4O_2P_8Si_4$	$C_{36}H_{107}B_2Li_2\ Mo_3N_3O_3P_{12}$	$C_{24}H_{86}B_5Li_5\ Mo_2N_2O_2P_8$
Color	Yellow-orange	Yellow	Yellow	Orange
Crystal dimensions (mm)	$0.36 \times 0.29 \times 0.10$	$0.36 \times 0.35 \times 0.13$	$0.48 \times 0.45 \times 0.42$	$0.52 \times 0.39 \times 0.16$
Temperature (K)	183(2)	123(2)	183(2)	173(2)
Crystal system	Triclinic	Monoclinic	Hexagonal	Triclinic
Space group (No.)	$P\bar{1}$ (2)	$P2_1$ (4)[b]	$P6_3/m$ (176)	$P\bar{1}$ (2)
a (Å)	9.7219(7)	37.963(3)	14.7234(8)	12.6227(10)
b (Å)	15.1842(11)	13.8403(6)	14.7234(8)	15.2542(12)
c (Å)	21.2454(15)	12.3531(7)	17.9738(13)	16.2615(13)
α (°)	87.380(8)	90	90	63.951(8)
β (°)	77.551(8)	92.773(7)	90	69.045(9)
γ (°)	73.894(8)	90	120	75.506(9)
V (Å^3)	2942.0(4)	6483.0(7)	3374.3(4)	2610.8(4)
Z	4	4	2	2
f_w	533.15	1189.10	1325.21	963.34
d (calc) (g cm^{-3})	1.204	1.218	1.304	1.225
Absorption coefficient (mm^{-1})	0.671	0.688	0.864	0.748
$F(000)$	1128	2512	1380	1008
2θ Scan range (°)	$4.46 < 2\theta < 55.90$	$3.22 < 2\theta < 45.24$	$6.40 < 2\theta < 60.78$	$5.42 < 2\theta < 60.58$
Number of unique data	13056	16136	3474	14159
Number of data observed [$I > 2\sigma(I)$]	6697	14172	1813	9858
Absorption correction	Numerical	Numerical	Numerical	Numerical
Solution method	Patterson	Patterson	Patterson	Patterson
Number of parameters refined	517	1042	88	536
R, wR_2 (%) all data	10.36, 8.07	5.90, 13.73	11.49, 19.50	5.83, 7.18
R_1, wR_2 (obsd) (%)[a]	4.71, 7.59	5.10, 13.11	7.47, 18.25	3.39, 6.58
Goodness-of-fit	0.992	1.053	1.038	1.011

[a] $R_1 = \sum(F_o - F_c)/\sum F_o$; $I > 2\sigma(I)$; $wR_2 = \{\sum w(F_o^2 - F_c^2)^2 / \sum w(F_o^2)^2\}^{1/2}$.
[b] Due to an unresolved twinning/disorder problem, structure **3** had to be determined in non-centrosymmetric equivalent of space group $P2_1/n$ (see text).

method using the program SHELXS-97 [21], and they were refined with SHELXL-97 [22]. For compound **3** racemic twinning was observed with Flack's x-parameter of 0.41(3) at convergence, the twin ratio was hence about 2:3. The X-ray data collections and the processing parameters are given in Table 5.

5. Supplementary material

CCDC 607142, 607143, 607144 and 607145 contain the supplementary crystallographic data for **2**, **3**, **4** and **5**. The data can be obtained free of charge via htpp://www.ccdc.cam.ac.uk/conts/retrieving.html, or from the Cambridge Crystallographic Data Centre, 12 Union Road, Cambridge CB2 1EZ, UK; fax: (+44) 1223-336-033; or e-mail: deposit@ccdc.cam.ac.uk.

Acknowledgments

Financial support from the Swiss National Science Foundation and the Funds of the University of Zurich is gratefully acknowledged.

References

[1] (a) C.P. Horwitz, D.F. Shriver, Adv. Organomet. Chem. 23 (1984) 219;
(b) D.F. Shriver, J. Organomet. Chem. 94 (1975) 259;
(c) M.Y. Darensbourg, Prog. Inorg. Chem. 33 (1985) 221.
[2] (a) G.B. Richter-Addo, P. Legzdins, Metal Nitrosyls, Oxford University Press, New York, 1992;
(b) G.B. Richter-Addo, P. Legzdins, Chem. Rev. 88 (1988) 991;
(c) F. Bottomley, Reactions of Nitrosyls, in: P.S. Braterman (Ed.), Reactions of Coordinated Ligands, vol. 2, Plenum, New York, 1989, p. 115.
[3] A.E. Crease, P. Legzdins, J. Chem. Soc., Dalton Trans. (1973) 1501.
[4] S. Onaka, Inorg. Chem. 19 (1980) 2132.
[5] P. Legzdins, S.J. Rettig, L. Sánchez, Organometallics 7 (1988) 2394.
[6] N.J. Christensen, A.D. Hunter, P. Legzdins, Organometallics 8 (1989) 930.
[7] K.E. Lee, A.M. Arif, J.A. Gladysz, Inorg. Chem. 29 (1990) 2885.
[8] A. Llamazares, G. Artus, H. Berke, in preparation.
[9] (a) P. Legzdins, S.F. Sayers, Organometallics 15 (1996) 3907;
(b) P. Legzdins, S.F. Sayers, Chem. Eur. J. 3 (1997) 1579;
(c) P. Legzdins, K.J. Ross, S.F. Sayers, S.J. Rettig, Organometallics 16 (1997) 190.
[10] F. Liang, H.W. Schmalle, H. Berke, (2006), in press.
[11] F. Liang, H.W. Schmalle, T. Fox, H. Berke, Organometallics 22 (2003) 3382.
[12] (a) M.F. Lappert, M.J. Slade, A. Singh, J. Am. Chem. Soc. 105 (1983) 302;
(b) L.M. Engelhardt, A.S. May, C.L. Raston, A.H. White, J. Chem. Soc., Dalton Trans. (1983) 1671.
[13] L.M. Engelhardt, B.S. Jolly, P.C. Junk, C.L. Raston, B.W. Skelton, A.H. White, Aust. J. Chem. 39 (1986) 1337.
[14] (a) A. Heine, D. Stalke, J. Organomet. Chem. 542 (1997) 25;
(b) H.-H. Giese, H. Nöth, H. Schwenk, S. Thomas, Eur. J. Inorg. Chem. (1998) 941–949.

[15] (a) D.R. Armstrong, W. Clegg, H.M. Colquhoun, J.A. Daniels, R.E. Mulvey, I.R. Stephenson, K. Wade, J. Chem. Soc., Chem. Commun. (1987) 630;
(b) H.-H. Giese, T. Habereder, H. Nöth, W. Ponikwar, S. Thomas, M. Warchhold, Inorg. Chem. 38 (1999) 4188;
(c) D.L. Reger, J.E. Collins, M.A. Matthews, A.L. Rheingold, L.M. Liable-Sands, I.A. Guzei, Inorg. Chem. 36 (1997) 6266;
(d) H.-H. Giese, T. Habereder, J. Knizek, H. Nöth, M. Warchhold, Eur. J. Inorg. Chem. (2001) 1195–1205.
[16] A.S. Antsyshkina, G.G. Sadikov, M.A. Porai-Koshits, V.N. Konoplev, T.A. Silina, A.S. Sizareva, Koord. Khim. 20 (1994) 274.
[17] J. Hooz, S. Akiyama, F.J. Cedar, M.J. Bennett, R.M. Tuggle, J. Am. Chem. Soc. 96 (1974) 274.
[18] C. Eaborn, M.N.A. El-Kheli, P.B. Hitchcock, J.D. Smith, J. Chem. Soc., Chem. Commun. (1984) 1673.
[19] D. Barr, M.J. Doyle, R.E. Mulvey, P.R. Raithby, D. Reed, R. Snaith, D.S. Wright, J. Chem. Soc., Chem. Commun. (1989) 318.
[20] Stoe IPDS software for data collection, cell refinement and data reduction. Version 2.87–2.92. Stoe & Cie, Darmstadt, Germany 1997–1999.
[21] G.M. Sheldrick, SHELXS-97, Acta Crystallogr. A 46 (1990) 467.
[22] G.M. Sheldrick, SHELXL-97: Programme for the Refinement of Crystal Structures, University of Göttingen, Germany, 1997.